Title

Precision ejection of microfluidic droplets into air with a superhydrophobic outlet

Permalink

https://escholarship.org/uc/item/7mf9s9bx

Journal

Lab on a Chip, 21(8)

ISSN

1473-0197

Authors

Zhang, Pengfei
Chang, Kai-Chun
Abate, Adam R

Publication Date

2021-04-20

DOI

10.1039/d0lc01327g

Peer reviewed

Precision ejection of microfluidic droplets into air with a superhydrophobic outlet

Pengfei Zhang[a], **Kai-Chun Chang**[a], **Adam R. Abate**[a,b,c,*]

[a]Department of Bioengineering and Therapeutic Sciences, University of California, San Francisco, San Francisco, CA, USA

[b]California Institute for Quantitative Biosciences, University of California, San Francisco, San Francisco, CA, USA

[c]Chan Zuckerberg Biohub, San Francisco, CA, USA

Abstract

Dispensing micron-scale droplets from a suspended nozzle is important for applications in bioprinting, analytical chemistry, and pharmaceutical formulation. Here, we describe a general approach to eject droplets from microfluidic devices using superhydrophobic patterning; this facilitates release of wetted fluids, allowing droplets to break contact with channel surfaces and travel along regular paths to achieve a printing accuracy of ~ 3 μm. We demonstrate the utility of the approach by using it to print droplets of varied composition from a microfluidic mixing device. Our approach is compatible with common fabrication techniques making it applicable to devices configured for diverse applications.

Graphical Abstract

We describe a general approach to controllably and precisely eject droplets of tunable composition from microfluidic devices using superhydrophobic patterning.
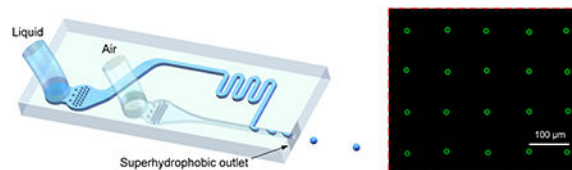
Introduction

Microfluidics allows controlled mixing, incubation, and analysis of fluids, with modern devices performing an array of chemical and biological functions, including separations,

---

[*]Correspondence to: adam@abatelab.org.

analyte detection, and single cell analysis.[1,2] A common challenge when applying microfluidics to a problem of interest is that, often, a specific measurement modality is required, but integrating it into the device is difficult. For example, in directed enzyme evolution, chemical assays must be used to quantify product formation,[3] while in single cell genomics, DNA must be analyzed with a sequencer.[4] A straightforward approach would be to process samples with the microfluidic devices, then dispense them onto a substrate for analysis. However, fluids are in physical contact with channel walls, so that ejecting them from devices requires overcoming capillary wetting forces that can be substantial at micron scales. Indeed, controlled ejection of droplets from a suspended channel is a common and important function in the use of fluidic devices throughout chemistry and biotechnology. For example, modern media printers dispense inks from piezo-actuated fluid reservoirs,[5] while flow cytometers eject liquid droplets from a suspended capillary to enable sorting.[6] Precision analytical techniques like inductively coupled mass spectrometry or X-ray Free Electron Laser spectroscopy disperse sample droplets into the analyzer or with a synchronized intercepting laser beam.[7,8]

Methods for ejecting droplets from microfluidic channels rely on breakup of unconfined liquid jets[7, 9–12] or pulsed ejection from a reservoir via application of physical, electromagnetic, or acoustic forces.[13–19] Jetting approaches yield uniform droplets, but cannot be rapidly shut off, making them unsuitable for applications requiring synchronization with external components. Actuation techniques can generate droplets of controlled size at defined times, but usually require that samples be maintained in specialized reservoirs that are difficult to integrate into microfluidic devices, like semiconductor ribbons in laser printing,[15] or hydrostatic fluid reservoirs for piezo actuation. [14,17] If an approach could be developed to controllably eject droplets from common microfluidic devices, it would allow a variety of measurement modalities to be utilized by processing the samples with the devices and then ejecting them as droplets onto an open substrate for analysis.

In this paper, we describe a general strategy to controllably eject droplets from microfluidic devices onto a substrate that can be subjected to additional analyses. The crucial feature is an outlet patterned to be superhydrophobic. This wetting property allows droplets in contact with channel surfaces to de-wet, thereby traveling in straight paths out of the device, to achieve a printing accuracy of ~3 μm. To demonstrate the approach, we use it to prepare and print droplets of distinct composition onto a grid that can be subjected to additional analyses, including imaging and mass spectrometry. Our approach provides a flexible means by which to controllably eject droplets from microfluidic devices.

Results and discussion

Modern microfluidics is dominated by glass and polymer devices fabricated with lithographic techniques, because they can be constructed with architectures tailored to diverse applications. However, due to the wetting properties of these devices, ejecting samples from them is challenging because it requires overcoming significant wetting forces. For example, the capillary force adhering a 50 μm water droplet to a PDMS channel wall is ~ 10,000 times that of gravity.[20] To enable controlled ejection of such droplets from a

microfluidic channel, we pattern the outlet to be superhydrophobic; this greatly reduces the capillary adhesion force and facilitates droplet release (Fig. 1a and Fig. S1a-c). The coating consists of PTFE nanoparticles with diameter of 200 – 300 nm applied as a spray (Fig. S2), ensuring near 100% of PDMS surface around the outlet to be coated; these particles are hydrophobic and the resultant coating has nanoscale roughness (Fig. 1b) rendering the surface superhydrophobic, with a contact angle of ~ 160°.

The wettability pattern is applied to the outer surface of the device, such that only this portion is superhydrophobic. The microchannel upstream of the outlet is native PDMS, with a contact angle of ~ 108°. While this surface is thus hydrophobic, with air as the continuous phase the aqueous droplets always remain wetted to the channel walls (Fig. S1d-e and Movie S1). Consequently, while droplet generation is reminiscent of a T junction with oil as the continuous phase, wetting forces alter the process and subsequent droplet motion. The rushing air shears the aqueous fluid at the T junction to ultimately pinch off a droplet. As the air continues to flow, it drags the droplet with a force $F_{drag} = \frac{1}{2}\rho\Delta v^2 A C_D$, where ρ is the density of air, v is the difference in velocity of the free-stream air flow and the sliding droplet, A is the frontal area of the deformed droplet facing air flow, and C_D is the drag coefficient.[21,22] Opposing the drag is adhesion of the droplet to the channel wall, $F_{adh} = kL_b\gamma_{ls}(\cos\theta_r - \cos\theta_a)$, where k is a parameter introduced to account for the distribution of contact angle of the noncircular contact line, L_b is the length of the droplet, γ_{ls} is the interfacial energy between the liquid and PDMS, and θ_r and θ_a are the receding and advancing contact angles, respectively. Provided $F_{drag} > F_{adh}$, the droplet moves down the channel (Fig. 1c and Fig. 2a).

Upon reaching the end of the channel, the anterior of the droplet approaches the superhydrophobic outlet, while the posterior portion remains attached to the inner surface of the channel (Fig. 2b). The flowing air stretches the droplet, resulting in one of three outcomes depending on air velocity. At low air velocity, the droplet wets the outer surface of the device and, consequently, no longer fully eclipses the air flow, coming to rest attached to the outlet (Fig. 2c$_1$, d$_1$, and e green dots). At moderate velocity, air drag is sufficient to fully de-wet the droplet and it maintains a straight trajectory out of the device (Fig. 2c$_2$, d$_2$, and e blue dots). At high velocity, air drag is higher than the interfacial tension force holding the droplet together,[23] so that a droplet rips off before complete dewetting, followed by eventual expulsion of the sister droplet (Fig. 2c$_3$, d$_3$, and e red dots). These outcomes can be understood by considering the air flow and droplet dynamics. As the droplet moves down the channel driven by the air flow, it builds kinetic energy; at the end of the channel, the shear stress elongates the droplet (Fig. 2d$_2$), increasing its surface energy.[24] With the elongated shape, the anterior of the droplet is unable to contact the outer superhydrophobic portion of the device, while the posterior portion continues forward driven by the air. If the air shear is too high, the elongated portion breaks off before the anterior fully de-wets (Fig. 2e red dots),[23] while if it is too low, the droplet's unelongated spherical shape allows it to contact the channel wall, where it remains wetted to the surface and does not detach (Fig. 2e green dots). By contrast, if the air shear is moderate, the droplet remains intact long enough for the posterior interface to reach the end of the channel, at which point the droplet fully de-

wets and is ejected (Fig. 2e blue dots). Thus, successful ejection of intact droplets occurs over a moderate range of air pressures and depends on the channel size (Fig. 2f).

When a device is set to eject intact droplets, size depends on the parameters of the T-junction and can be varied by adjusting flow rates (Fig. 3, Movie S2). As in a usual T junction, at high carrier flow rates (high air pressure) small droplets are formed rapidly (Fig. 3a) of uniform size (inset in Fig. 3a). As carrier pressures are reduced, larger droplets are formed more slowly (Fig. 3b). Thus, for a given channel size, monodispersed droplets of controlled diameter can be generated by tuning the air pressure (Fig. 3a). To generate droplets over a larger diameter range, bigger or smaller channels can be used, with each device having its optimal range. The droplet generation is inherently fast, with a lower limit of ~100 Hz and upper of 3,000 Hz for the devices tested (Fig. 3b). A factor that uniquely limits the maximum rate at which uniform droplets can be ejected from the device is that detachment at the outlet is slow compared to droplet generation at the T junction. Hence, if droplets are generated too rapidly they collide at the outlet, thereby being ejected as a merged droplet. The surface tension of the aqueous phase impacts its ability to wet the outlet, with lower surface tensions being harder to eject. We determine that surface tensions beyond ~ 47 mN m^{-1} yield reproducible ejection, and that droplet size slightly increases with surface tension (Fig. S3). Notably, within this range, droplet size slightly decreases with increasing viscosity.

The direction that the droplet travels after ejection depends on the air flow rate, because the droplet is wetted to only one channel surface, yielding a flow asymmetry at the outlet (Fig. 4a). At low air pressures, droplets tend to travel in the same direction as the longitudinal axis of the channel, while at higher pressures, they are deflected away from this axis (Fig. 4a, inset). This allows ejection angle to be controlled over a limited range. Moreover, for fixed air pressure, the angle is stable, with a variation of ~ 0.5° over about 1 h (Fig. 4b).

In certain applications, droplet ejection must be synchronized with another event, such as substrate movement or a laser pulse. T junction drop formation, however, generates droplets in a continuous stream and cannot be rapidly turned on and off, making it difficult to synchronize with other components. To enable this, we thus implement sorting to deliver droplets on demand[25] (Fig. 5a-b); when registered with the substrate, this allows controlled printing of micropatterned arrays (Fig. 5c). Sorting is achieved by staining the droplets with fluorescent dye (FITC) enabling them to be detected as they travel past embedded fibers (Fig. 5a, red-orange bars). If droplets should not be dispensed, the sorting electrode is activated, generating a dielectrophoretic force that deflects them into a waste channel. Alternatively, if a droplet should be dispensed, the electrode is deactivated, so that it travels undeflected to the substrate. To print an array, we supply the control computer with instructions of the locations at which to print the droplets; the computer translates the substrate to each location, dispensing droplets according to the file. Due to the small variation of ejection angle and close proximity with which the device can be brought to the substrate (~3 mm), droplets can be printed with an accuracy of ~3 μm (Fig. 5d-e), which is more precise than previously reported microfluidic droplet ejectors.[14,19,25] The printable area is limited by the travel of the substrate positioning stage, with a bigger stage allowing larger print areas.

Existing approaches for printing droplets do not employ microfluidic pre-processing and, thus, are unable to tune composition during the printing process.[14,15,17] This capability is valuable for a variety of applications, including patterning chemical and biological materials or measuring the kinetics of fast catalysts.[26,27] A unique and valuable property of our approach is that the ejection strategy is applicable to microfluidic architectures that can be uniquely configured to process the sample prior to droplet printing into an open-air environment, which is not possible with conventional printers. To illustrate this, we construct a device that mixes distinct liquids at varying ratios, then prints them as droplets to the substrate (Fig. 6a). The volumetric ratio of the fluids in the droplets is proportional to their flow rate ratio in the device, which can be precisely controlled; moreover, since mixing conditions are registered to the substrate by on-demand printing, the composition of every printed droplet is controlled and known (Fig. 6b and 6c). By adding additional inlets controlled by valves,[28] this device can print droplets selected from a combinatorial space.

Conclusions

We describe a flexible approach to controllably eject droplets from microfluidic devices. Our approach uses a T junction to disperse samples into droplets that are subsequently ejected from an outlet into air. To facilitate de-wetting of the droplet and control ejection angle, we pattern the outlet to be superhydrophobic which, as we show, allows droplets to reliably detach from channel surfaces. Our approach is implemented in polymer devices fabricated using lithographic techniques and, thus, should be applicable to a broad array of architectures to enable controlled dispensing from these devices.

Transferring droplets to an open substrate allows analysis of microfluidically processed samples with techniques that are normally difficult to utilize in microfluidic workflows, because they cannot be easily integrated into the devices. Moreover, the approach is compatible with high-speed droplet sorting, thereby allowing droplets to be dispensed on demand. This allows synchronization of dispensing with other components, such as analytical instruments or substrate printing. By incorporating other components into the microfluidic device to mix and process fluids, including membrane valves,[28] separators,[29] and analyte concentrators,[30] this should allow printing of arrays with distinct but controlled features. For example, characterizing the rates of chemical and enzyme-based reactions is important in analytical biochemistry, but often requires specialized instruments that can prepare and rapidly analyze samples.[31] These instruments are tailored specifically for the task and cannot be easily altered with additional functionality. Using our approach, different microfluidic architectures can be integrated into a device that prepares the solution and prints it onto the substrate, whereupon they dry and the reaction stops; the substrate can then be analyzed using a variety of techniques, such as imaging and spectroscopy, to quantify reaction kinetics. Because droplets are delivered on demand to defined positions, the processing history of each printed droplet can be recovered and associated to the subsequent measurement. Alternatively, the approach can be used to load nanoliter well plates with reagents for applications in quantitative toxicity analysis.

The ultimate limit to dispensing precision of our approach is the distance that the droplets must travel after ejection, over which small errors in deflection angle grow. Because our

device can be fabricated with lithographic techniques, it holds potential to allow all components to be further miniaturized, which would allow travel distance to be reduced and, thus, even higher printing accuracy. Our approach provides a flexible strategy to address numerous technical challenges in microfluidics and substrate printing.

Experimental Section

Device fabrication

The microfluidic devices were fabricated using soft lithography. Masters were fabricated from SU-8 on a 3-inch silicon wafer via photoresist (3025, MicroChem, Westborough, MA, USA) using standard photolithography. Pre-cured Polydimethylsiloxane (PDMS, RTV 615, Momentive, Waterford, NY, USA) with prepolymer and curing agent ratio of 10:1 were poured onto the masters, degassed in a vacuum chamber, and baked in an oven at 65°C for 4 h. These PDMS slabs were extracted from the masters and punched using a 0.75-mm biopsy core. The structured PDMS slabs were bonded onto flat PDMS after oxygen plasma treatment (Plasma Cleaner, Harrick Plasma). The devices were baked in the oven at 65°C for 2 days to render the channels hydrophobic.

Superhydrophobic outlet preparation

A spray-coating method was employed to prepare the superhydrophobic surface around the outlet (Fig. S2). PTFE nanoparticles (Microdispers-200, Polysciences, USA) with diameter of 200–300 nm were suspended in HFE oil (mass ratio: 1:15) to prepare coating solutions. Before spray-coating, solutions were ultrasonicated for 10 min. About 10 uL of coating solutions were deposited onto PDMS surface around the outlet. Airflow from the outlet prevented solutions from wetting into the channel. The coating solutions were then dried by an air sprayer. The coated devices were baked in an oven at 65°C for 30 min. Superhydrophobic surfaces were characterized by SEM (Sigma 500).

Droplet formation characterization

Air flow rate was controlled using an air flow controller (900X, Control Air Inc., NH) and custom LabVIEW interface. Liquids were injected into the device using a syringe pump (New Era, Farmingdale, NY). For diameter analysis, droplets were ejected into oil (Novec HFE-7500, 3M, supplemented with 0.2% wt/wt biocompatible surfactant) and transferred to a counting slide (Countess, Invitrogen) using a pipette, followed by imaging using a fluorescence microscope (EVOS, ThermoFisher). A high-speed camera (Phantom Miro M-310, Vision Research) monitored droplet formation and ejection. Water was mixed with ethanol to obtain liquids with different surface tensions.

Droplet printing

The device was modified to an on-demand droplet printer by implementing a fluorescence activated droplet sorter using a previously described approach.[25] Optical fibers (Thorlabs, Newton, NJ) with a cladding diameter of 225 μm, an optical core diameter of 200 μm, and an NA of 0.22 were coated with liquid metal and inserted into respective channels for laser delivery. Liquids were stained with FITC or Cy5 with a final concentration of 5 μM and excited by a 473 or 638 nm laser. The printing process was automated by a custom

LabVIEW interface. The printing substrates were placed on an XY mechanical stage (MA-2000, ASI, Eugene, OR) which was automatically controlled by the software. During printing, the sorting electrode was charged with ~ 2 kV via a high voltage amplifier (690E-6, Trek, Lockport, NY). Deflected droplets were collected into tubing and vacuumed to waste. Controlled printing was achieved by selecting droplets according to pre-programmed instructions.

Supplementary Material

Refer to Web version on PubMed Central for supplementary material.

Acknowledgements

References

[1]. Teh SY, Lin R, Hung LH and Lee AP, Lab Chip, 2008, 8, 198–220. [PubMed: 18231657]

[2]. Shang L, Cheng Y and Zhao Y, Chem. Rev, 2017, 117, 7964–8040. [PubMed: 28537383]

[3]. Gielen F, Hours R, Emond S, Fischlechner M, Schell U and Hollfelder F, Proc. Natl. Acad. Sci. U. S. A, 2016, 113, 7383–7389. [PubMed: 27382153]

[4]. Lan F, Demaree B, Ahmed N and Abate AR, Nat. Biotechnol, 2017, 35, 640–646. [PubMed: 28553940]

[5]. Demirci U and Montesano G, Lab Chip, 2007, 7, 1139–1145. [PubMed: 17713612]

[6]. Picot J, Guerin CL, Le Van Kim C and Boulanger CM, Cytotechnology, 2012, 64, 109–130. [PubMed: 22271369]

[7]. Verboket PE, Borovinskaya O, Meyer N, Günther D and Dittrich PS, Anal. Chem, 2014, 86, 6012–6018. [PubMed: 24805360]

[8]. Knoška J, Adriano L, Awel S, Beyerlein KR, Yefanov O, Oberthuer D, Murillo GEP, Roth N, Sarrou I, Villanueva-Perez P and Wiedorn MO, Nat. Commun, 2020, 11, 657. [PubMed: 32005876]

[9]. Trebbin M, Krüger K, DePonte D, Roth SV, Chapman HN and Förster S, Lab Chip, 2014, 14, 1733–1745. [PubMed: 24671443]

[10]. Amstad E, Gopinadhan M, Holtze C, Osuji CO, Brenner MP, Spaepen F and Weitz DA, Science, 2015, 349, 956–960. [PubMed: 26315432]

[11]. Visser CW, Kamperman T, Karbaat LP, Lohse D and Karperien M, Sci. Adv, 2018, 4, eaao1175. [PubMed: 29399628]

[12]. Mäeots ME, Lee B, Nans A, Jeong SG, Esfahani MM, Ding S, Smith DJ, Lee CS, Lee SS, Peter M and Enchev RI, Nat. Commun, 2020, 11, 3465. [PubMed: 32651368]

[13]. Ferraro P, Coppola S, Grilli S, Paturzo M and Vespini V, Nat. Nanotechnol, 2010, 5, 429–435. [PubMed: 20453855]

[14]. Bsoul A, Pan S, Cretu E, Stoeber B and Walus K, Lab Chip, 2016, 16, 3351–3361. [PubMed: 27444216]

[15]. Vinson BT, Sklare SC and Chrisey DB, Curr. Opin. Biomed. Eng, 2017, 2, 14–21.

[16]. Castro JO, Ramesan S, Rezk AR and Yeo LY, Soft Matter, 2018, 14, 5721–5727. [PubMed: 29845144]

[17]. Mao Y, Pan Y, Li X, Li B, Chu J and Pan T, Lab Chip, 2018, 18, 2720–2729. [PubMed: 30014071]

[18]. Castro JO, Ramesan SR, Dang HD, Rezk AR and Yeo LY, Anal. Chem, 2019, 91, 5621–5628. [PubMed: 30915842]

[19]. Brenker JC, Devendran C, Neild A and Alan T, Lab Chip, 2020, 20, 253–265. [PubMed: 31854405]

[20]. Ismail AE, Grest GS, Heine DR, Stevens MJ and Tsige M, Macromolecules, 2009, 42, 3186–3194.

[21]. Milne AJB and Amirfazli A, Langmuir, 2009, 25, 14155–14164. [PubMed: 19685896]

[22]. Moghtadernejad S, , Tembely M, , Jadidi M, , Esmail N and Dolatabadi A, Phys. Fluids, 2015, 27, 032106.

[23]. Amstad E, Spaepen F, Brenner MP and Weitz DA, Lab Chip, 2017, 17, 1475–1480. [PubMed: 28294220]

[24]. Lee DJ, Kim HM, Song YS and Youn JR, ACS Nano, 2012, 6, 7656–7664. [PubMed: 22928700]

[25]. Zhang P and Abate AR, Adv. Mater, 2020, 32, 2005346.

[26]. Shakeri A, Imani SM, Chen E, Yousefi H, Shabbir R and Didar TF, Lab Chip, 2019, 19, 3104–3115. [PubMed: 31429455]

[27]. Olivon K and Sarrazin F, Chem. Eng. J, 2013, 227, 97–102.

[28]. Ochs CJ and Abate AR, Lab Chip, 2015, 15, 52–56. [PubMed: 25385230]

[29]. Lan W, Liu D, Guo X, Liu A, Sun Q, Li X, Jing S and Li S, Ind. Eng. Chem. Res, 2020, 59, 12262–12269.

[30]. Kopp MR, Linsenmeier M, Hettich B, Prantl S, Stavrakis S, Leroux JC and Arosio P, Anal. Chem, 2020, 92, 5803–5812. [PubMed: 32249573]

[31]. Gielen F, Van Vliet L, Koprowski BT, Devenish SR, Fischlechner M, Edel JB, Niu X, Demello AJ and Hollfelder F, Anal. Chem, 2013, 85, 4761–4769. [PubMed: 23614771]
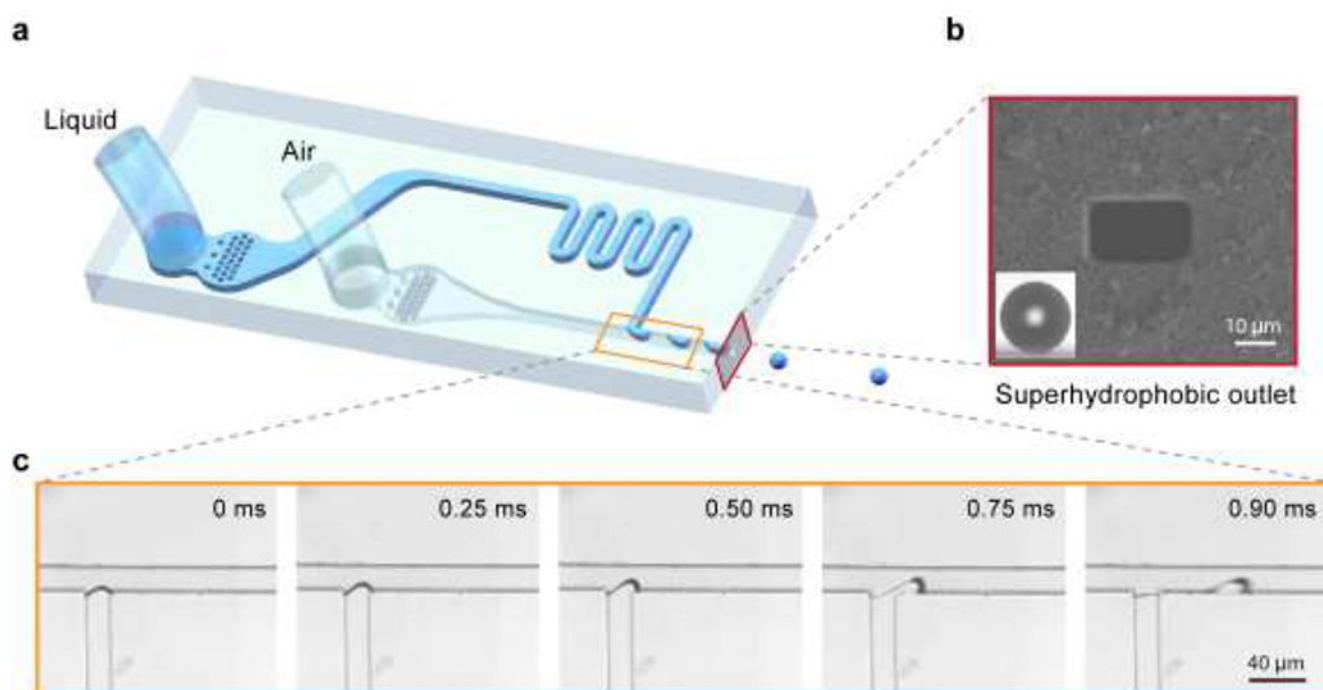
Fig. 1. Device design and operation.

(a) Schematic of microfluidic device for generating droplets in air that are ejected from the outlet. (b) The outlet is pattered with PTFE nanoparticles to render it superhydrophobic, with a contact angle of ~ 160° (inset); this wettability facilitates release of droplets from the device. (c) Time-lapsed images showing droplet formation at the T junction.
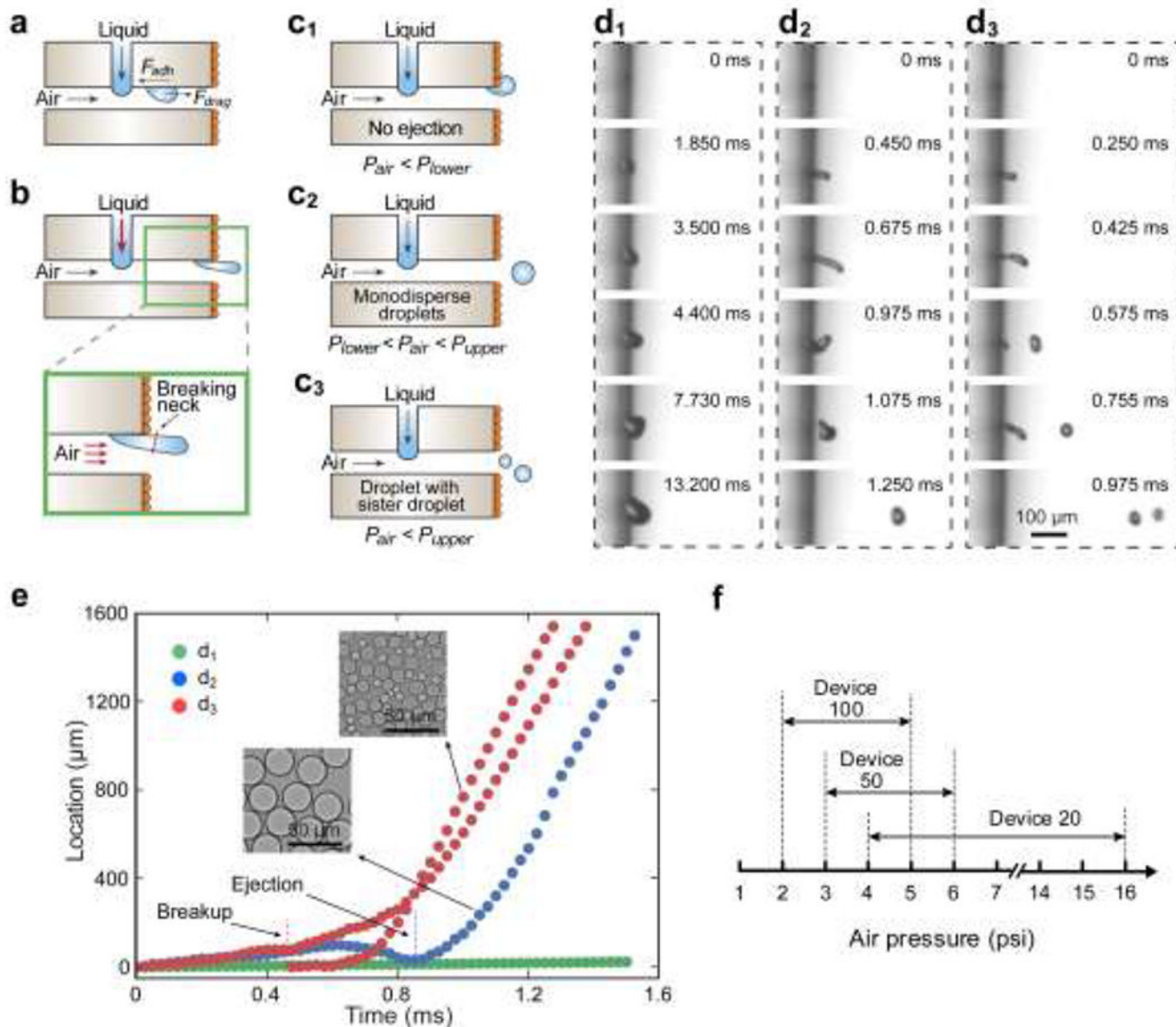
Fig. 2. Droplet ejection dynamics.
Schematic of droplet ejection with (a) droplet sliding in channel driven by air shear and (b) droplet ejected at the outlet due to wetting inhibition by the superhydrophobic patterning. Ejection dynamics depend on the applied air pressure: (c_1) no ejection occurs when the air pressure is below a lower critical value; (c_2) monodispersed droplets are ejected when the air pressure is within a moderate range; (c_3) droplets are split when the air pressure is above an upper critical value. Time-lapsed images of droplet ejection for (d_1) no ejection, (d_2) monodispersed droplets, and (d_3) split droplets. (e) Droplet location from the outlet versus time; the insets show representative droplets. (f) The air pressure range with successful droplet ejection for the devices used in this work. Device 20, device 50, and device 100 indicate the devices with ejection channel size of 19×26 μm, 49×54 μm, and 101×113 μm, respectively.
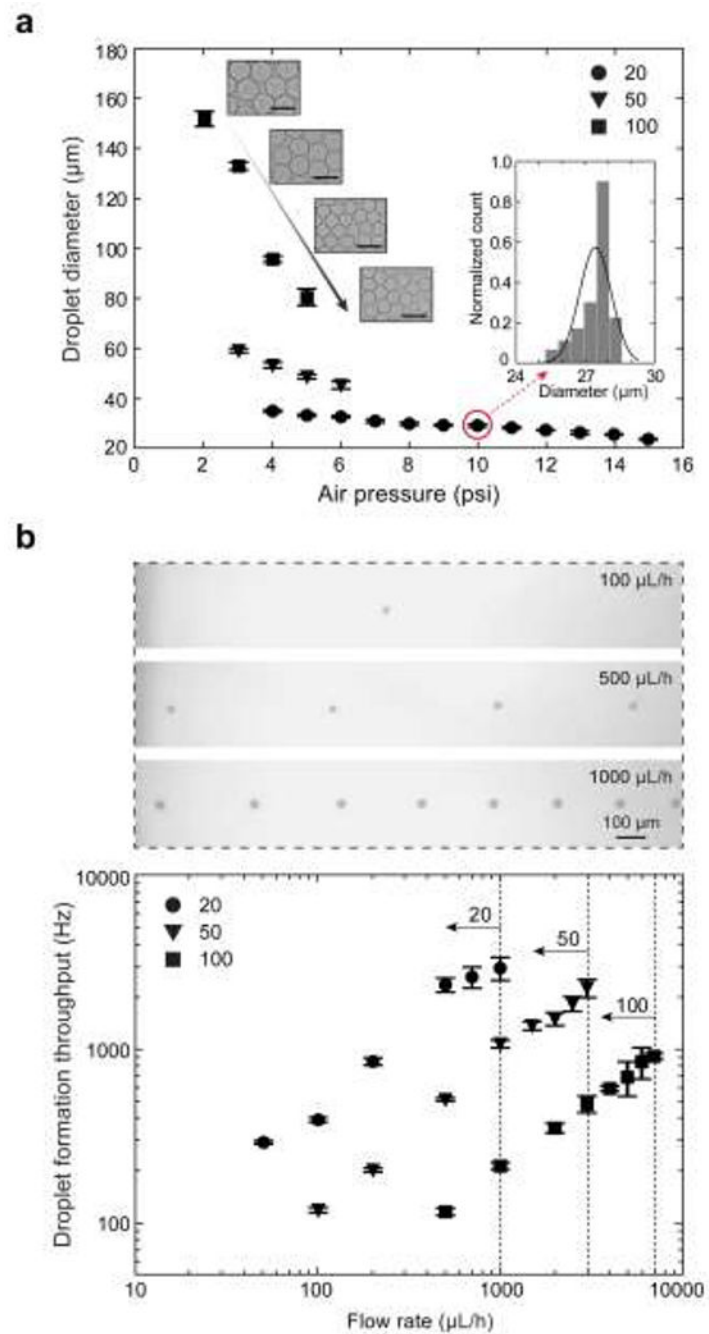
Fig. 3. Controlling droplet formation.
(a) Variation of droplet diameter with different channel sizes as a function of air pressure. Histogram (inset) shows a representative droplet diameter distribution. 20, 50, and, 100 indicate the devices with ejection channel size of 19×26 μm, 49×54 μm, and 101×113 μm, respectively. Scale bars represent 200 μm. (b) Upper images show droplets ejected with different liquid flow rates for Device 20 at air pressure of 10 psi. Variation of droplet formation throughput with different channel sizes as a function of liquid flow rate.
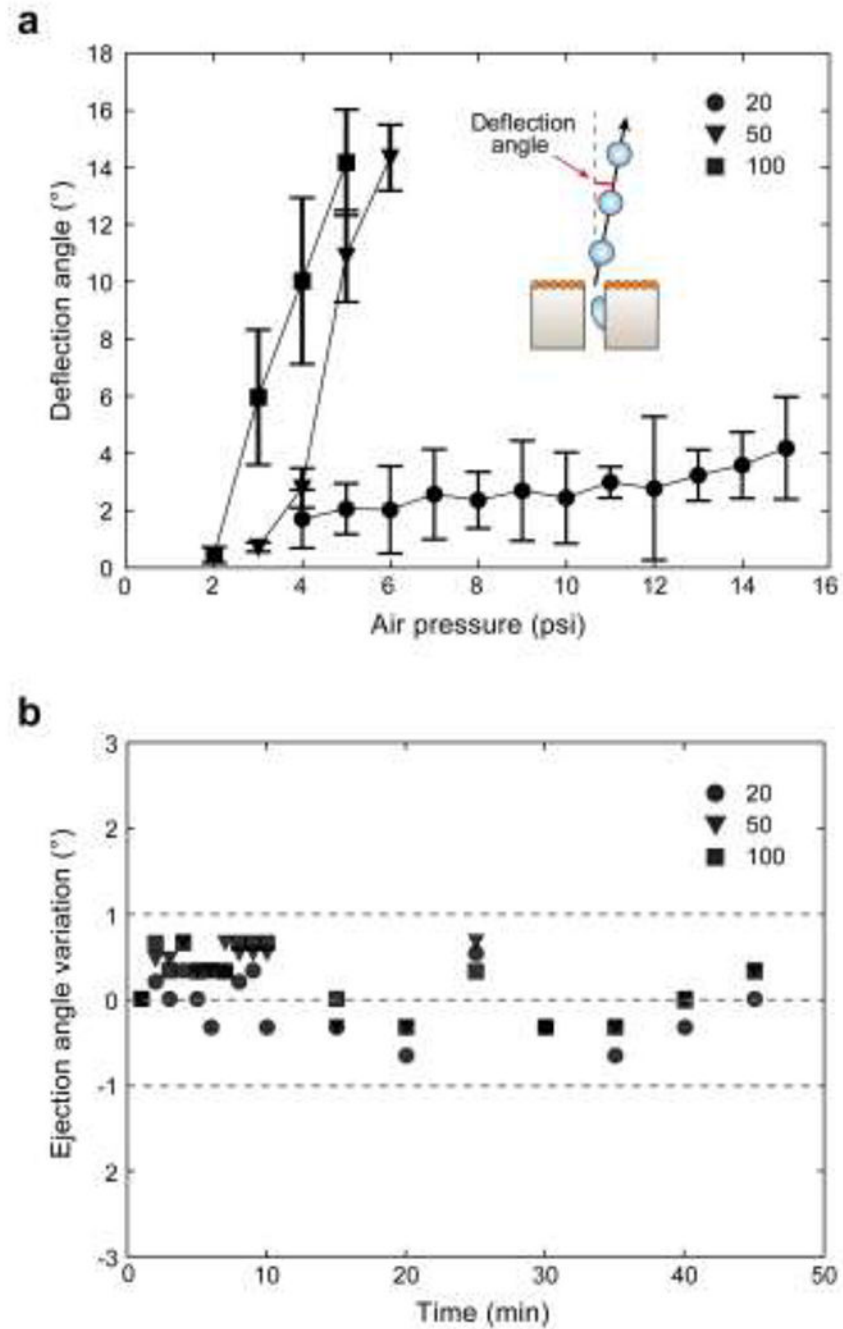
Fig. 4. Controlled droplet ejection.
(a) Variation of droplet deflection angle after ejection with different channel sizes versus air pressure. (b) Time-dependence of droplet ejection angle.
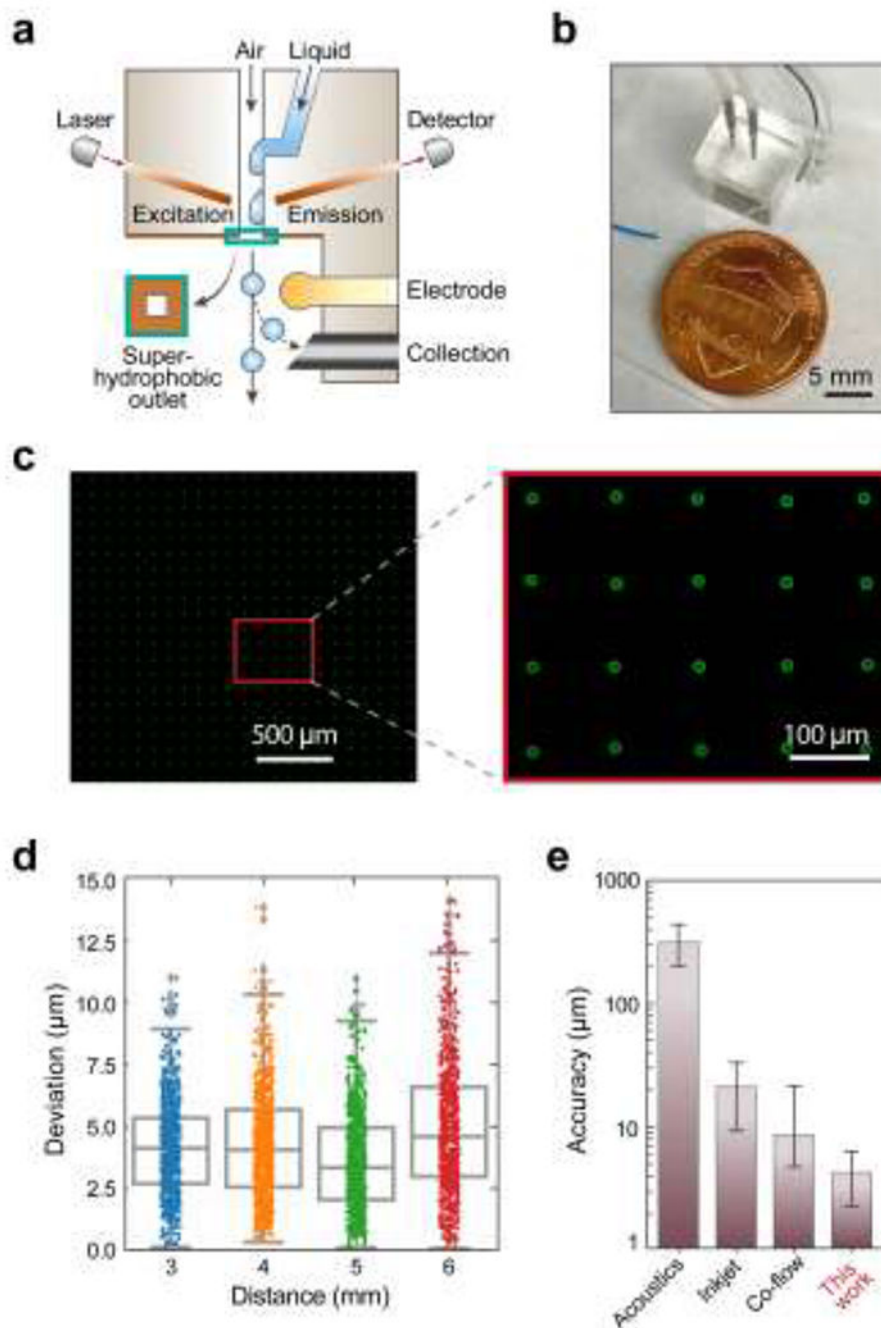
Fig. 5. On-demand high-accuracy droplet printing.
Schematic (a) and photograph (b) of on-demand droplet ejection device. (c) Printed single droplet array (left) with enlarged image (right). (d) Variation of printed droplet deviation with respect to the theoretical position as a function of printing distance, showing a mean accuracy of 3-4 μm for a printing distance of 3-5 mm. (e) Printing accuracy based on different microfluidic designs. Data of acoustics are adapted from reference [19], data of inkjet are adapted from reference [14], and data of co-flow are adapted from reference [25].
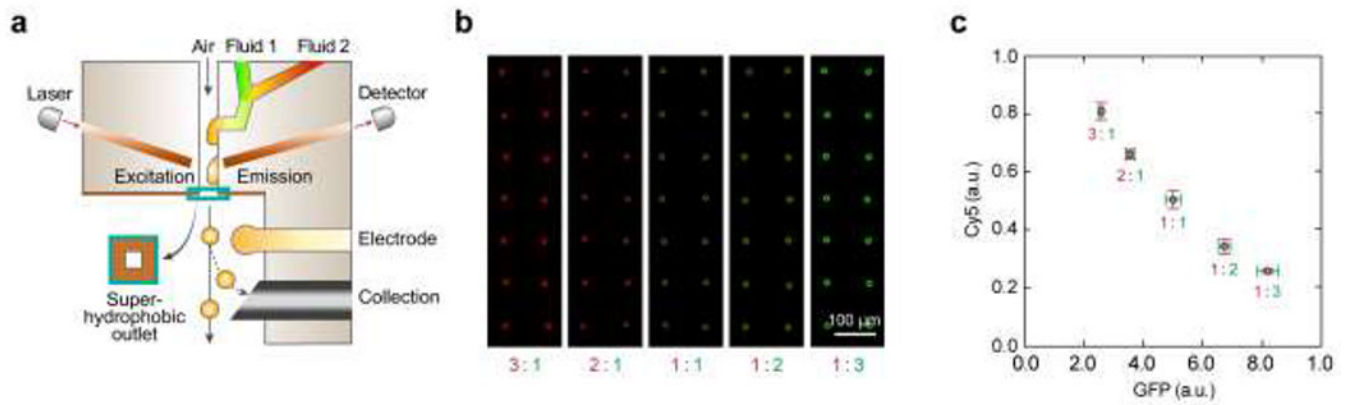
Fig. 6. Droplet printing with tunable composition.
(a) Schematic of microfluidic device for mixing and printing different liquids. Droplet composition can be tuned by controlling the ratio of Liquid 1 and Liquid 2. (b) Printed droplets from mixing FITC stained liquid (green) and Cy5 stained liquid (red) at different mixing ratios. (c) Plot of fluorescence intensity for droplets printed at different mixing ratios in (b).